Chapter 1

State-of-the-Art and Perspectives of Geometric and Implicit Modeling for Molecular Surfaces

Giuseppe Patané and Michela Spagnuolo

Abstract This paper reviews state-of-the-art methods and presents new perspectives of implicit modeling, together with their relations with Constructive-Solid-Geometry, for the computation and analysis of molecular surfaces. The link between implicit modeling techniques and the generation of molecular surfaces is possible thanks to the representation of the molecule as the iso-surface of an implicit function and to the definition of the solvent-accessible/solvent-excluded surfaces as the union/intersection of atoms. We also review methods that consider the position of each atom as a probability distribution and introduce new representations of molecular surfaces based on the uncertainty and thermal vibration of the atoms. Finally, the specialization of implicit modeling techniques to molecular surfaces allows us to analyze geometric/topological properties of molecules; to address molecular docking through the identification of cavities; and to combine surface-based and volume-based information through the implicit representation of the electron density map.

1.1 Introduction

The correct representation of molecular surfaces is fundamental for their processing, analysis, and visualization. However, multiple connected components, spurious cavities or holes, and topological inconsistencies generally affect the current representations of molecular surfaces. A locally incorrect representation of molecules, which is due to inherent pathologies in the classical definition of the van der Walls, solvent-accessible and solvent-excluded surfaces, badly influences the classification

Giuseppe Patané · Michela Spagnuolo
CNR-Consiglio Nazionale delle Ricerche, IMATI-Istituto di Matematica Applicata e Tecnologie Informatiche, Via De Marini, 6, 16149 Genova, Italy e-mail: {patane,spagnuolo}@ge.imati.cnr.it

of its features, the identification of docking sites, and the evaluation of local similarities among molecules. These geometric and topological artifacts in the representation of the molecular surfaces [1] are also due to the resolution of the voxel grid, on which the electrostatic field is sampled to extract the molecular surface through Marching Cubes [13] or alternative algorithms [9]; local perturbations in the computed samples of the electron density map; numerical errors; and a limited approximation accuracy. Indeed, the definition of a correct representation of the molecular surface is still crucial to correctly simulate the mutual interactions of molecules and the understanding of biological phenomena.

This paper reviews state-of-the-art methods and presents new perspectives of implicit modeling, together with their relations with Constructive-Solid-Geometry (CSG), for the computation and analysis of molecular surfaces. The link between implicit modeling techniques with the generation and analysis of molecular surfaces is possible thanks to the representation of the molecule as the iso-surface of an implicit function and to the definition of the solvent-accessible/solvent-excluded surfaces as the union/intersection of atoms. Our interest on implicit surfaces for molecular representation is also motivated by the possibility of extracting differential properties (e.g., normals, normal and principal curvatures) of the molecule directly from the underlying implicit representation; computing set-theoretic operations (e.g., union, intersection, subtraction, off-setting) through functional operations; imposing interpolation/smoothness constraints on the surface through different implicit representations based on radial basis functions and moving least-squares approximation. The application of implicit modeling techniques to the case of molecular surfaces allows us to analyze geometric/topological properties of molecules, to address molecular docking through the identification of cavities, and to combine surface-based and volume-based information through the implicit representation of the electron density map.

The blobby model and the CSG-based model for the generation of the molecular surface assume that the position of the atom is fixed in space and that there is no thermal vibration of the atoms and no uncertainty in the determination of their position. However, the atom position is fuzzy as a matter of the uncertainty in the protein structure determination and the thermal vibration of the atoms. The spatial organization of the atoms determines the bio-molecular properties of the molecule and its surface is mainly defined by the force fields of the atoms, whose thermal vibration determines rapid changes of the surface. To address these issues, we review methods that consider the position of each atom as a probability distribution and introduce new representations of molecular surfaces based on the uncertainty and thermal vibration of the atoms.

This chapter is organized as follows. Firstly (Sect. 1.2), we introduce the molecular surface representations with implicit functions through blobby models for the computation of the volume electron density map and multi-resolution methods. Then, we apply constructive solid geometry techniques (Sect. 1.3), thermal vibration and uncertainty (Sect. 1.4) in the representation of molecules. We also characterize molec-

ular cavities for docking and artifacts in the representation of molecules (Sect. 1.5). Finally (Sect. 1.6), we discuss open issues and future work.

1.2 Molecular surface representations with implicit functions

The representation of the molecular surface is crucial to correctly simulate the mutual interactions of molecules and the understanding of biological phenomena. Among the different molecular surfaces, we recall the *van der Walls surface*, which is the boundary of the spheres representing the atoms of the molecules; the *solvent accessible surface*, which is defined as the boundary of the van der Walls spheres whose radii have been increased by the radius of the solvent molecule; and the *solvent excluded surface*, which is the surface that is traced out by rolling the solvent molecule over the solvent accessible surface. Here, the solvent molecule (i.e., a water molecule) is typically represented as a sphere and is used to localize the ligand binding site; in fact, the ligand is capable of accessing all the sites that are reachable by a water molecule. Then, the *molecular surface* includes the part of the van der Walls surface that is accessible to a probe sphere (*contact surface*) and the inward surface of the probe when it touches two or more atoms (*reentrant surface*). Generally, van der Walls surfaces are not capable of accurately describing the molecular surface behavior, due to the overestimation of the surface in molecular dynamics or to the incorrect encoding of the length of ionic and covalent bounds. Molecular interfaces are determined by atomic and molecular interactions, which are also influenced by other physical phenomena in a neighborhood of the molecular surface.

This richness in the definition of the molecular surface highlights the difficulty in the identification of a mathematical representation of this surface, which is crucial to correctly simulate the mutual interactions of molecules and the understanding of biological phenomena. To address this issue, we focus our attention on implicit representations of surfaces (Sect. 1.2.1), which are successively specialized to the class of molecules (Sect. 1.2.2). The aim of these definition is to provide a reliable representation the molecular surface, which resembles specific local properties of the surface itself. However, a unique definition of the molecular surface, which combines all its main properties, is still missing.

1.2.1 Implicit representation of surfaces

To introduce implicit modeling in a general context, let $f : \mathbb{R}^d \to \mathbb{R}$ be a continuous function. For instance, we can consider $d := 3$ (i.e., the Euclidean 3D space) and select f as the implicit function underlying the blobby model (Sect. 1.2.2), which is

commonly used to generate the molecular surface. Then, the function f defines the implicit solid $\mathscr{S} := \{\mathbf{x} \in \mathbb{R}^d : f(\mathbf{x}) \geq 0\}$ as the set of points of $\mathbb{R}^d$ whose f-values are greater than or equal to zero. The function f also identifies two half spaces on which f is strictly positive or negative and the boundary $f^{-1}(0)$ of these two solids is the level-set associated to the null iso-value. If $f \in \mathscr{C}^2$ and it has no critical points (i.e., $\nabla f \neq \mathbf{0}$), then the iso-surfaces $\mathscr{S}_\alpha := f^{-1}(\alpha)$ related to different iso-values α are well-defined, closed, and free of self-intersections. They also identify implicit solids with different geometric (e.g., area, volume) and topological properties (e.g., number of connected components, genus).

The usefulness of implicit representations is due to the possibility of (i) extracting differential properties (e.g., normals, normal and principal curvatures) of the iso-surface directly from the underlying implicit representation; (ii) computing set-theoretic operations (e.g., union, intersection, subtraction, off-setting) through functional operations; (iii) imposing different constraints on the surface properties, such as interpolation of points and smoothness conditions, through different implicit representations based on radial basis functions and moving least-squares approximations.

According to the underlying function, implicit surfaces are classified into three main groups: algebraic surfaces, globally- and locally-defined implicit surfaces. *Algebraic surfaces* are defined by a polynomial implicit function; in this case, we represent only simple surfaces, such as planes, spheres, cylinders, etc. *Global implicit representations* are expressed as a linear combination of a set of basis functions; among them, we mention blobby models and implicit representations with radial basis functions. Blobby models are commonly used for the generation of the electron density map underlying the molecular surface and radial basis functions are useful to interpolate and/or approximate a set of function values sampled at 3D points. *Local implicit representations* approximate the input data in a neighborhood of the sample point and locally adjust the implicit function to the approximation accuracy, thus reducing the computational cost for sampling the implicit function on a regular grid.

Global and local approximation of molecular properties Choosing a kernel $\varphi : \mathbb{R}^+ \to \mathbb{R}$, the volumetric approximation $F : \mathbb{R}^3 \to \mathbb{R}$ of a discrete set of properties represented as the vector $\mathbf{f} := (f_i)_{i=1}^n$ is defined as a linear combination $F(\mathbf{x}) := \sum_{i=1}^n \alpha_i \varphi_i(\mathbf{x})$ of the radial basis functions $\varphi_i(\mathbf{x}) := \varphi(\|\mathbf{x} - \mathbf{x}_i\|_2)$ centered at $\{\mathbf{x}_i\}_{i=1}^n$. Then, the coefficients $\alpha := (\alpha_i)_{i=1}^n$, which uniquely satisfy the interpolating conditions $F(\mathbf{x}_i) = f_i$, $i = 1, \ldots, n$, are the solutions of the $n \times n$ square linear system $\mathbf{A}\alpha = \mathbf{f}$, where the entries of the matrix $\mathbf{A}$ are $a_{ij} := \varphi(\|\mathbf{x}_i - \mathbf{x}_j\|_2)$. In case of noisy data, interpolating conditions are replaced by least-squares constraints. Depending on the properties of φ and of the corresponding approximation scheme, we distinguish globally-supported [3, 24] and compactly-supported [25, 15, 17] radial basis functions, and the partition of unity [16, 27]. Globally-supported kernels are associated to full coefficient matrices, which require a prohibitive storage and computational cost with respect to compactly-supported kernels. Selecting compactly-

supported basis functions generally provide sparse coefficient matrices and a lower computation cost.

As an alternative to the global approximation schemes previously introduced, the moving least-squares approximation [8, 12] defines a local approximation scheme that is adapted to both the local distribution of points and the f-values. To this end, a weight $W(\mathbf{x},\mathbf{x}_i)$ is associated to each point $\mathbf{x}_i$ with respect to $\mathbf{x}$ and a weighted least-squares energy is minimized. Since the weight function $W(\cdot,\cdot)$ rapidly decreases to zero, in the approximation we consider only the f-values at those points $\mathscr{N}_\mathbf{x} := \{\mathbf{x}_{j_s}\}_{s=1}^k$ of $\mathbf{x}$, which includes those points of $\mathscr{P}$ that fall inside the sphere of center $\mathbf{x}$ and radius $\sigma(\mathbf{x})$. Here, the value $\sigma(\mathbf{x})$ is chosen according to the local sampling density of $\mathscr{P}$ [22]. Then, we search the approximation $F : \mathbb{R}^3 \to \mathbb{R}$ in the linear space of polynomial lower than a certain degree r (e.g., $r := 2,3$), thus solving a linear system whose size is proportional to the degree of the polynomials that are reproduced by the method. This choice makes the approximation scheme *local*; guarantees a $\mathscr{O}(r^3)$ cost for the evaluation of $F(\mathbf{x})$; avoids to sample every basis function φ_i at $\mathbf{x}$; and improves the conditioning number of the coefficient matrix of the corresponding normal equation.

1.2.2 Blobby model and volume electron density map

We introduce the blobby model and its specialization to the definition of the electron density map for molecular surface representation. Then, we discuss the multiresolution representation of molecular surfaces, which is useful to encode the local/global features and make the computation faster, also reducing the inflation of the molecular surface due to Gaussian maps.

Blobby model The implicit function underlying the blobby model [2] is defined as a linear combination of maps $\varphi_i(\mathbf{x}) := \varphi(\|\mathbf{x}-\mathbf{x}_i\|_2/\sigma_i)$, generated by a decreasing kernel $\varphi : \mathbb{R}^+ \to \mathbb{R}$ and centered at the points $\mathbf{x}_i$, $i = 1,\ldots,n$; i.e.,

$$G(\mathbf{x}) := \sum_{i=1}^{n} \alpha_i \exp(-\beta_i \varphi(\|\mathbf{x}-\mathbf{x}_i\|_2)). \tag{1.1}$$

In this representation, the parameter α_i controls the strength of the map φ_i in $G(\cdot)$ and β_i controls its decay degree. Common choices are the Gaussian $\varphi(t) := \exp(-t)$ and the multi-quadratic $\varphi(t) := \sqrt{t^2+c^2}$, $c > 0$, kernels. Since the Gaussian maps exponentially tend to zero as we move far from their centers, in the evaluation of Eq. (1.1) we consider only the contribution of those functions whose centers are close to the evaluation point $\mathbf{x}$. The resulting implicit surface is smooth, free of singularities and self-intersections, and allows us to analytically compute geometric surface properties, such as normals and curvature.

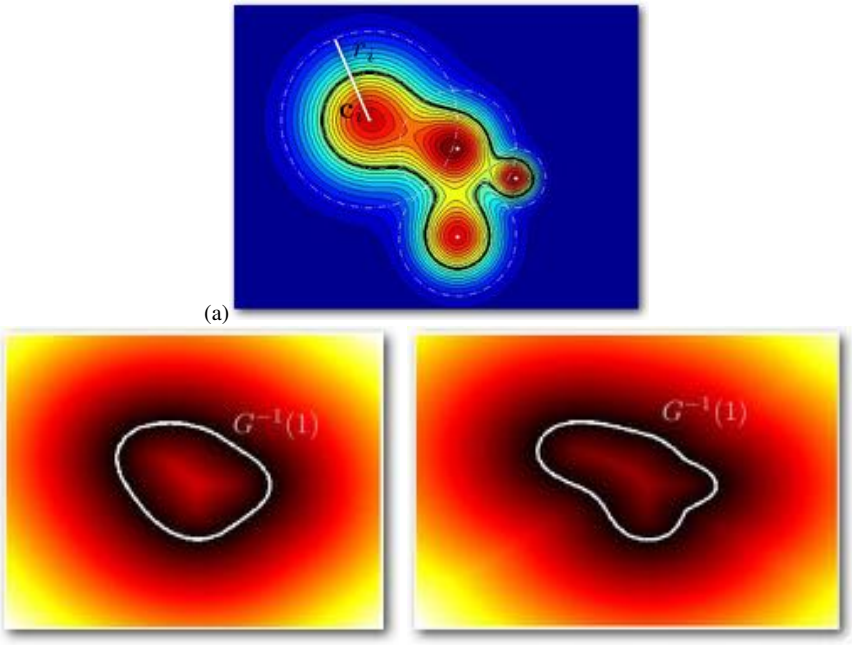

(a) (b) $B := -1$ (c) $B := -2$

Fig. 1.1: ***Electron density map and molecular surface.*** *(a) Iso-curves of the electron density $G(\cdot)$ in Eq. (1.2) on the plane and generated by 5 atoms (white points) with different radii. Color coding of the values of $G(\cdot)$ on a rectangle that contains the atoms and corresponding iso-curves; (black) level-set related to the iso-value 1 mimics the molecular surface. (b,c) The behavior of $G(\cdot)$ and the shape of the corresponding level-set $G^{-1}(1)$ depend on the centers, radii, and the selected decay factor.*

Electron density map and molecular surface representation The blobby model is specialized to molecular surfaces by considering only a constant decay and a negative constant strength. Then, the molecular surface (*implicit solvation surface*) is represented as the iso-surface $\mathscr{S} := G^{-1}(1)$ of the *volumetric electron density map* [28], which is defined as a linear combination of Gaussian functions centered at the atoms $(\{\mathbf{c}_i, r_i)\}_{i=1}^n$ of the molecule; i.e.,

$$G(\mathbf{x}) := \sum_{i=1}^{n} \exp\left[B\left(\frac{\|\mathbf{x}-\mathbf{c}_i\|_2}{r_i^2}\right) - 1\right]. \tag{1.2}$$

The Gaussian basis functions, whose constant B controls both the decay and the strength of the function $G(\cdot)$, identify the atomic density and recall the spherical atomic orbitals. Indeed, this representation is a special case of the blobby model (1.1); here, the selection of the blobby value B is related to the size of the solvent

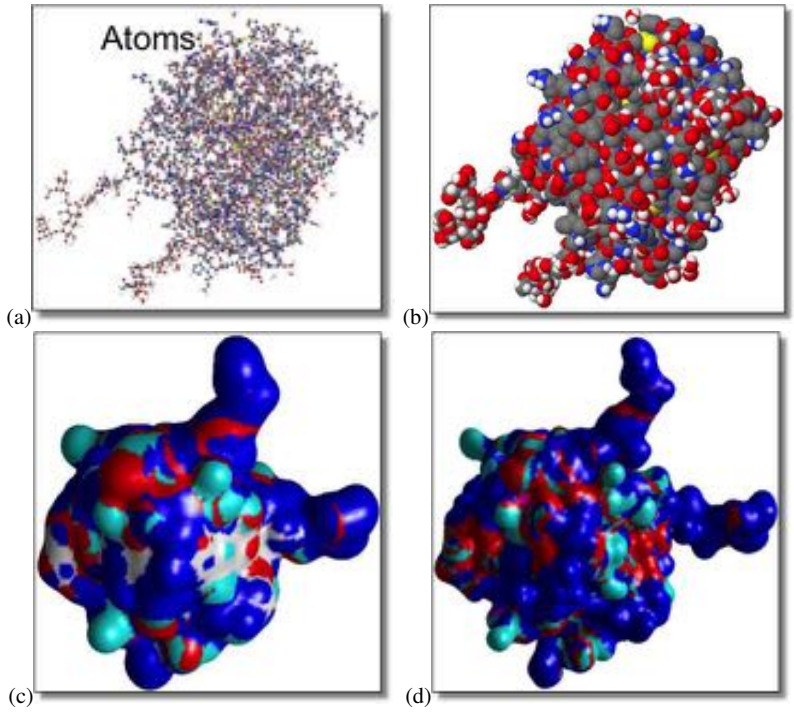

Fig. 1.2: ***Multi-resolution representation of molecular surfaces.*** *(a, b) Input atoms and (c,d) multi-resolutive hierarchy of atoms computed by clustering their centers according to criterion of the minimal distance. Molecular surface at two levels of detail in the hierarchy. (c) Low resolution level; several atoms have been clustered and only the global structure of the molecular surface is reconstructed. (d) Residue-level resolution, where we represent smaller details through the selection of a higher number of atoms. Each molecular surface has been computed using the Marching Cubes method; the values of the electron density map have been computed using the blobby model (1.2) and have been sampled on a regular grid.*

probe and influences the energy estimation of the molecular system (Fig. 1.1). For values of B close to $-\infty$ or 0, the density map tends to a constant. To extract the molecular surface, we apply the Marching Cubes method [13] to the values of the electron density map sampled on a regular or an adaptive grid and extract the molecular surface as the iso-surface $\mathscr{S} := \{\mathbf{x} \in \mathbb{R}^3 : G(\mathbf{x}) = 1\}$ related to the iso-value 1 (Fig. 1.2).

We briefly discuss the main pro and cons of blobby models for the representation of molecular surfaces. Blobby models conform to the stability of the chemical structure of the atoms, recall the spherical representation of the orbits of the atoms, and disregard the thermal vibration of atoms. They also provide a simple representa-

tion of the electron density map as a linear combination of a set of Gaussian basis functions centered at the atoms, which are sampled at any point and are efficiently evaluated to identify the inner and outer part of the molecular surface. Furthermore, the electron density map is differentiable and the resulting iso-surface is free of self-intersections and singularities. However, models of the electrostatic potential fields [6] are more accurate and computationally more expensive than blobby models. Since they are usually rasterized through partial differential equations on a regular grid, local changes to the grid generally require to recompute the whole solution. On the contrary, for blobby models it is only necessary to sample the electron density map at the new sample points with a linear computational cost.

Multi-resolution representation of the molecular surface For the efficient computation of the blobby model, multi-resolutive methods [28] reduce the inflation of Gaussian basis functions and the computational cost for sampling the electron density map at the nodes of the volumetric grid, which depends on the number of atoms and the grid size. To this end, atoms are hierarchically clustered according to proximity criteria: at each level of the hierarchy, spheres are clustered in a priority queue on the basis of a local error estimation and clustered spheres are replaced by a new sphere. At the next level, the centre and radius of this new sphere is determined in such a way that the new sphere encloses the clustered spheres (Fig. 1.2). The error estimation for the generation of the priority queue takes into account the Euclidean distance among the centers of the atoms that are clustered; the variation of the area and volume of the generated molecular surface at each level of detail in the multi-resolutive hierarchy; the Hausdorff distance between clustered atoms and molecular surface. In this way, the molecular surface is encoded with a varying resolution and the resulting multi-resolutive hierarchy allows us to identify its global structure and local details.

1.3 Constructive solid geometry for molecular surface representation

We now discuss how geometrical operations on solids are converted to operations on the corresponding implicit representations; then, we specialize these results to the computation of the molecular surface.

Constructive solid geometry with implicit surfaces We have previously mentioned that an implicit function identifies an implicit solid. We now define set-theoretic operations [23], such as union, intersection, and subtraction, using min/max operations or evaluating analytic representations. To this end, let us consider two implicit solids $\mathscr{S}_1$, $\mathscr{S}_2$ defined by the implicit functions f_1, f_2. Then, their union is represented as the implicit solid associated to the function $f := \max\{f_1, f_2\}$. In a similar way, the union operation is associated to the function $f := \min\{f_1, f_2\}$ and the subtraction $\mathscr{S}_1 \setminus \mathscr{S}_2$ is identified by the map $\min\{f_1, -f_2\}$ (Fig. 1.3(c-e)).

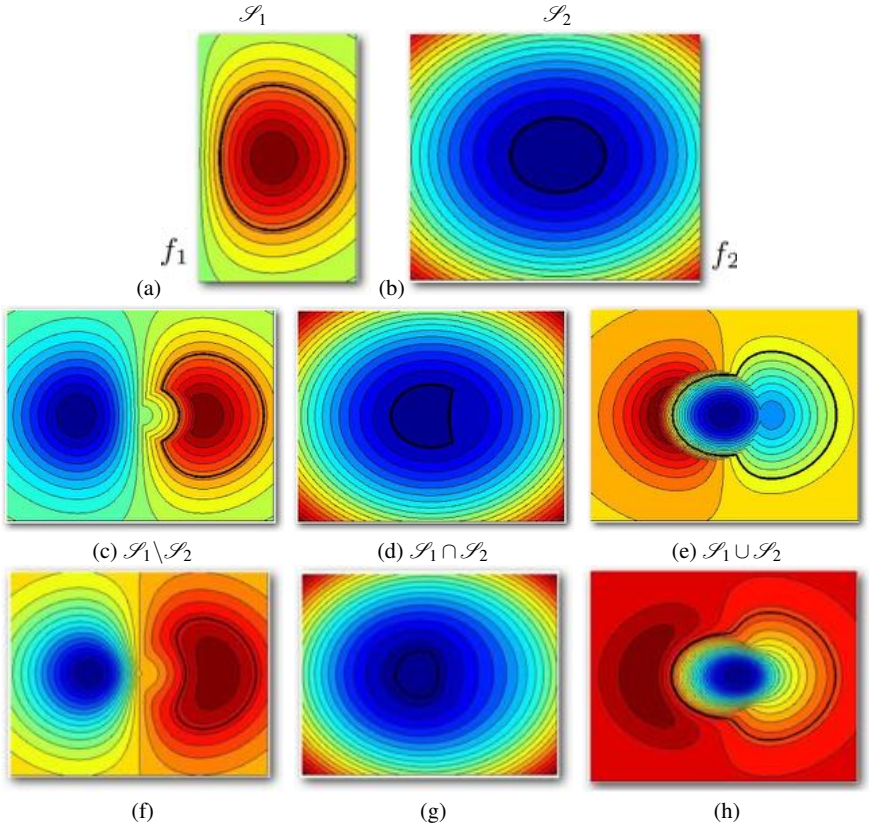

Fig. 1.3: ***Constructive Solid Geometry operations on curves defined by implicit maps.*** *(a, b) Implicit (black) curves $\mathscr{S}_1$, $\mathscr{S}_2$ defined as the level-set of f_1, f_2 with iso-value* 0*. (c-e) Behavior of the union, intersection, and subtraction of $\mathscr{S}_1$, $\mathscr{S}_2$ (black curves) computed applying the* min*,* max *operators to f_1, f_2. An example of $\mathscr{C}^1$ discontinuity is present at the intersection between $\mathscr{S}_1$ and $\mathscr{S}_2$. (f-h) Analytic approximations (1.3) of the previous operations.*

Alternatively [21], smooth versions of the set theoretic operations are defined through the following analytic representations of the min/max operators as (Fig. 1.3(f-h))

$$\begin{cases} \mathscr{S}_1 \cup \mathscr{S}_s \to [f_1 + f_2 + (f_1 + f_2 - 2f_1 f_2)], \\ \mathscr{S}_1 \cap \mathscr{S}_s \to [f_1 + f_2 - (f_1 + f_2 - 2f_1 f_2)]; \end{cases} \tag{1.3}$$

in particular $\mathscr{S}_1 \backslash \mathscr{S}_s = \mathscr{S}_1 \cap \mathscr{S}_2^C$, where $\mathscr{S}_2^C$ is induced by $-f_2$. The use of min/max and analytic representations of set-theoretic operations for implicit solids have the following analogies and differences. Set-theoretic operations based on min/max are only continuous with a $\mathscr{C}^1$ discontinuity when f_1 is equal to f_2. Set-theoretic operations based on analytic representations have a $\mathscr{C}^1$ smoothness but requires a higher

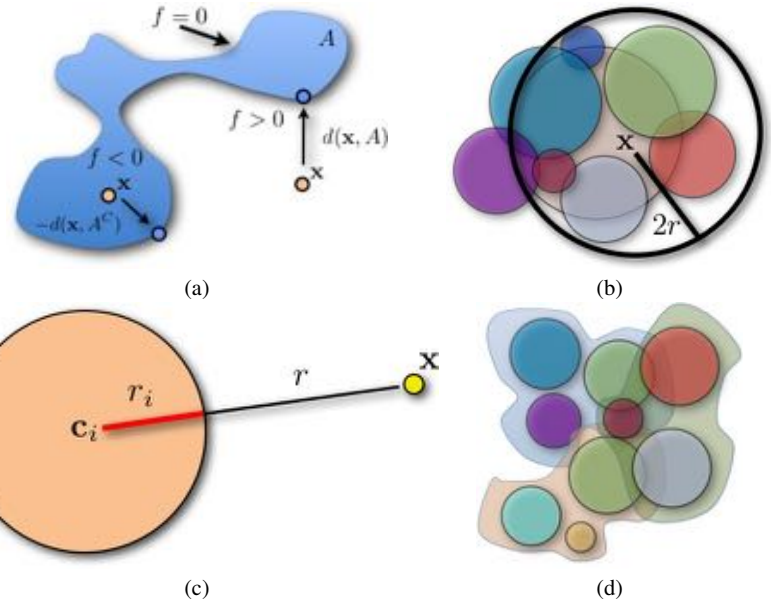

Fig. 1.4: ***Main steps for the definition of the implicit function underlying the molecular surface through CSG operations.*** *(a) Sign changes of the implicit function underlying the molecular surface. (b) Identification of the atoms* $\{(\mathbf{c}_i, r_i)\}_{i\in|\mathscr{S}|}$ *that belong to the sphere of centre* $\mathbf{x}$ *and radius* $2r$*. (c) Definition of the function* $f_i(\mathbf{x}) := r + r_i + \|\mathbf{x} - \mathbf{c}_i\|_2$ *centered at the atom* $(\mathbf{c}_i, r_i)$ *and used for the evaluation of the map* $f_{SAS}(\mathbf{x}) = \min_{i=1,\ldots,|S|}\{f_i(\mathbf{x})\}$ *underlying the solvent accessible surface. (d) Clustering of the atoms, according to the criterion of the minimal distance.*

computational cost. For molecular surface representation, the previous min/max or analytic representations are generally enough to generate a molecular surface of good geometric quality.

We now discuss the link between set-theoretic operations and the generation of the molecular surface, which is related to the following properties: (i) the molecular surface is represented by an implicit function that bounds an implicit solid; (ii) the solvent accessible surface and the solvent excluded surface can be defined as the union/intersection of the atoms of the molecule and the probe radius.

Constructive solid geometry for molecular surface representation Applying CSG operations, we define the solvent accessible surface and the solvent excluded surface through intersection and union of solids, thus using the set-theoretic operations and the corresponding function representations. More precisely [20], we locally define a smooth implicit function $f : \mathbb{R}^3 \to \mathbb{R}$ such that (Fig. 1.4(a))

- $f(\mathbf{x})$ is the point-to-set distance between $\mathbf{x}$ and the solvent excluded surface;

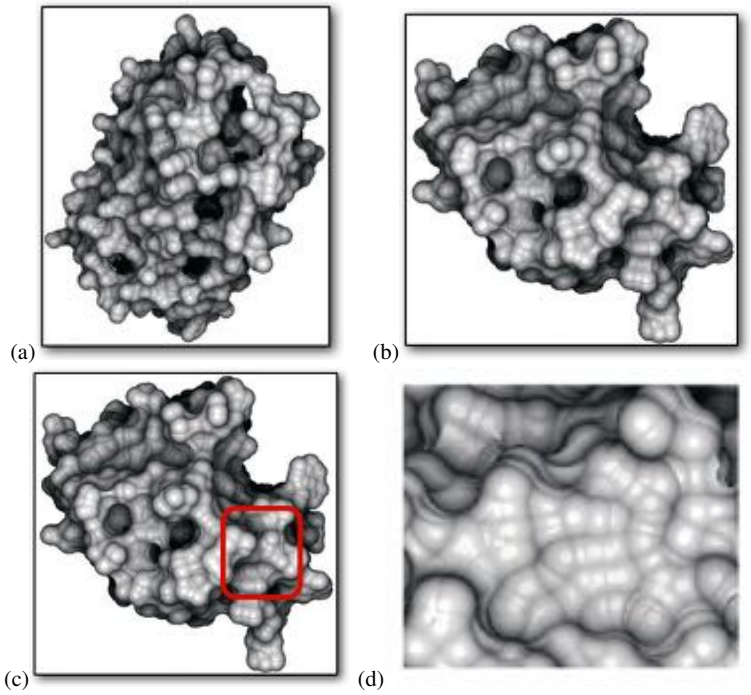

Fig. 1.5: ***CSG-based computation of molecules.*** *(a-c) Molecular surfaces computed with set-theoretic operations, which guarantees the surface continuity. (d) Zoom-in. Image courtesy of [20].*

- $f(\mathbf{x}) = 0$ if $\mathbf{x}$ belongs to the molecular surface;
- $f(\mathbf{x})$ is strictly positive or negative if $\mathbf{x}$ is outside or inside the surface, respectively.

The idea behind the proposed approach is to apply a local version of the blobby model; where the locality is measured with respect to the sample point. More precisely, the implicit function $f_{SAS}(\cdot)$ underlying the solvent accessible surface at $\mathbf{x}$ is computed by summing the contribution of those atoms $\{(\mathbf{c}_i, r_i)\}_{i \in |\mathscr{S}|}$ that belong to the sphere of centre $\mathbf{x}$ and radius $2r$ (Fig. 1.4(b)). According to the functional representation of set-theoretic operations, this function is computed by applying the min operator; i.e., $f_{SAS}(\mathbf{x}) = \min_{i=1,\ldots,|S|}\{r + r_i + \|\mathbf{x} - \mathbf{c}_i\|_2\}$ (Fig. 1.4(c,d)). In a similar way, the solvent excluded surface at $\mathbf{x}$ is computed by subtracting the union of spheres centered at the previous set of atoms from the solvent accessible surface; i.e., we apply the set-theoretic operations and we get (Fig. 1.5)

$$f_{SES}(\mathbf{x}) = f_{SAS}(\mathbf{x}) - \bigcup_{\mathbf{y} \in f_{SAS}^{-1}(0)} (R - \|\mathbf{x} - \mathbf{y}\|_2)\,.$$

These two surfaces are computed using the union, intersection, and subtraction of implicit solids through min/max operations or their smooth approximation Eq. (1.3).

1.4 Thermal vibration and uncertainty for molecular surface representation

A correct identification of the boundary between the solvent and the solute is crucial to guarantee an accurate and stable computation of the solution to the Poisson-Boltzman equation. On the one hand, the spatial organization of the atoms determines the bio-molecular properties of the molecule. On the other hand, the molecular surface is mainly defined by the force fields of the atoms, whose thermal vibration determines rapid changes of the surface. The blobby model and the CSG-based model for the generation of the molecular surface assume that the position of the atom is fixed in space and that there is no thermal vibration of the atoms and no uncertainty in the determination of the atoms. However, the atom position is fuzzy as a matter of the uncertainty in the protein structure determination and the thermal vibration of the atoms.

According to [11], the idea is to consider the position of each atom as a probability distribution; a natural choice is the Gaussian distribution. Collecting the probability distributions of all the atoms, we compute the likelihood volume as the probability that an atom is at a given location. In this way, atoms in stable conditions are still represented as spheres and dynamic configurations are represented as a range of positions of the atoms themselves. To encode the thermal vibration and uncertainty in the blobby model, these two terms are modeled with a Gaussian distribution

$$G(\mathbf{x}) := \left[\frac{\Sigma^{-1}}{(2\pi)^3} - \frac{1}{2}\mathbf{x}^\top \Sigma^{-1}\mathbf{x} \right]^{1/2},$$

where Σ is the mean-squares displacement matrix. Assuming also that the thermal vibration and the uncertainty are isotropic, the mean-squares displacement matrix is diagonal and the Gaussian distribution is $G(\mathbf{x}) = (2\pi\sigma)^{-3/2}\exp(-(2\sigma)^{-1}\|\mathbf{x}\|_2)$. Because each atom has an arbitrary centre and radius, we represent the distribution in homogeneous coordinates as $G(\mathbf{x}) = (2\pi\sigma)^{-3/2}\left(-(2\sigma)^{-1}\|\mathbf{M}\mathbf{x}\|_2^2\right)$, where $\mathbf{x}$ is the 4×4 homogeneous 3D transformation matrix for an atom. With reference to Fig. 1.6(a), regions of the two Gaussian graphs with the same area have equal probability to find the two atoms within distance σ_1 and σ_2 from their mean center.

Then, the p-probability sphere for an atom $\mathscr{A}$ is defined as the smallest sphere that contains the center of $\mathscr{A}$ with probability p and the fuzzy molecular surface is the collection of p-probability surfaces defined using a set of spheres each of that encloses atoms with the same probability. The p-probability sphere for an atom $\mathscr{A}$ is the smallest sphere that contains the center of $\mathscr{A}$ with probability p and the *fuzzy*

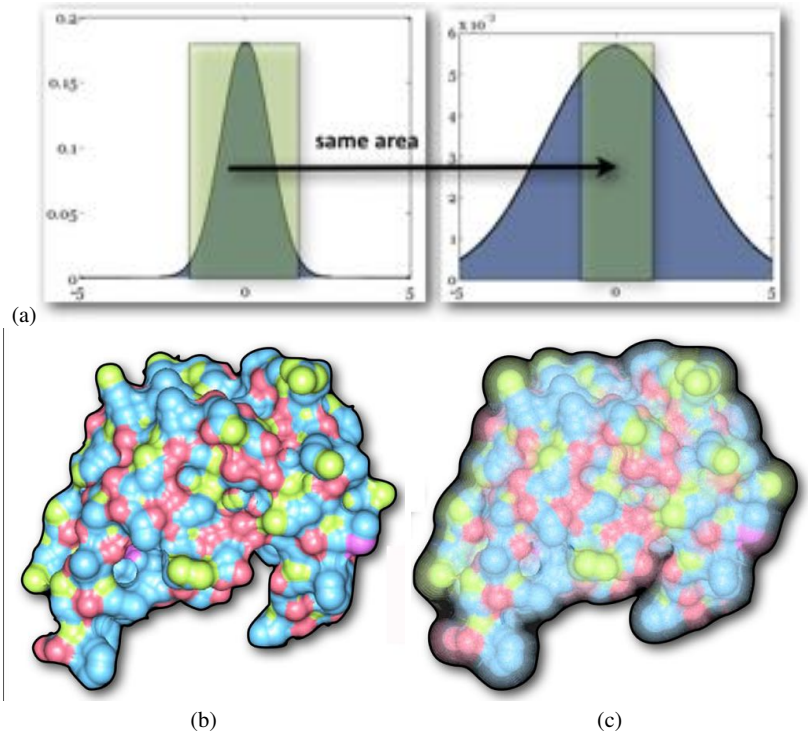

Fig. 1.6: ***Blobby and fuzzy molecular surfaces.*** *(a) Gaussian probability distribution of two atoms. Regions of the two graphs with the same area have equal probability to find the two atoms within distance σ_1 and σ_2 from their mean center. If $\sigma_1 > \sigma_2$, then atom $\mathscr{A}_1$ has a greater fuzziness (i.e., more vibration/uncertainty) than $\mathscr{A}_2$. Comparison between the (b) blobby and (c) fuzzy molecular surfaces. Images (b,d) are courtesy of [11].*

molecular surface is defined as the collection of *p*-probability surfaces defined using a set of spheres each of that encloses atoms with the same probability. These new basis functions are used to insert the information related to the uncertainty of the positions of the atoms (Fig. 1.6(c)) in the definition of the electron density map underlying the blobby model (Fig. 1.6(b)).

1.5 Characterization of the molecular surface

We have previously pointed-out that an implicit function identifies an implicit solid and set-theoretic operations can be converted to function representations. We now

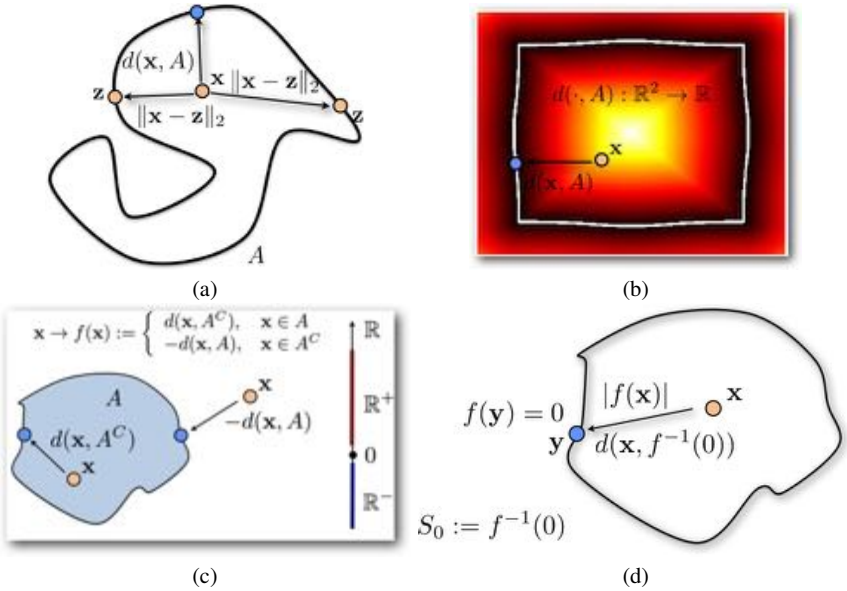

Fig. 1.7: ***Point-to-set distance.*** *(a) Definition and (b) example of the point-to-set distance from the (white) curve $\mathscr{A}$. (c) Signed point-to-set-distance. (d) Relation between $f(\mathbf{x})$ and the distance between $\mathbf{x}$ and the level-set $f^{-1}(0)$.*

show that any closed set in $\mathbb{R}^d$ can be represented as the level-set of an implicit function associated to the null iso-value. This function is the point-to-set distance (Sect. 1.5.1), which will be used for the identification of cavities in molecular surfaces (Sect. 1.5.2); in fact, it provides a simple way to establish if a point is inside or outside the molecular surface by simply checking its sign or the variation of its sign.

1.5.1 Point-to-set distance for local shape characterization

The *point-to-set distance* of a point $\mathbf{x}$ to the closed set $\mathscr{A}$ of $\mathbb{R}^d$ is defined as the minimum distance of $\mathbf{x}$ from $\mathscr{A}$; i.e., $d(\mathbf{x}, \mathscr{A}) := \min_{\mathbf{y} \in \mathscr{A}} \{\|\mathbf{x}-\mathbf{y}\|_2\}$ (Fig. 1.7(a)). Since we are evaluating the minimum of a continuous function (i.e., the Euclidean distance) from a closed set (i.e., $\mathscr{A}$), we have that this minimum exists and is unique. By definition, all the points of $\mathscr{A}$ have null point-to-set distance from $\mathscr{A}$; i.e., $\mathscr{A}$ is the level-set associated to the null iso-value of the implicit function defined as the point-to-set distance from $\mathscr{A}$ (Fig. 1.7(b)). The resulting surface depends on the quality of the discrete sampling and its local geometry; in fact, the distance map has a linear behavior when the sample point is close to the surface and the surface curva-

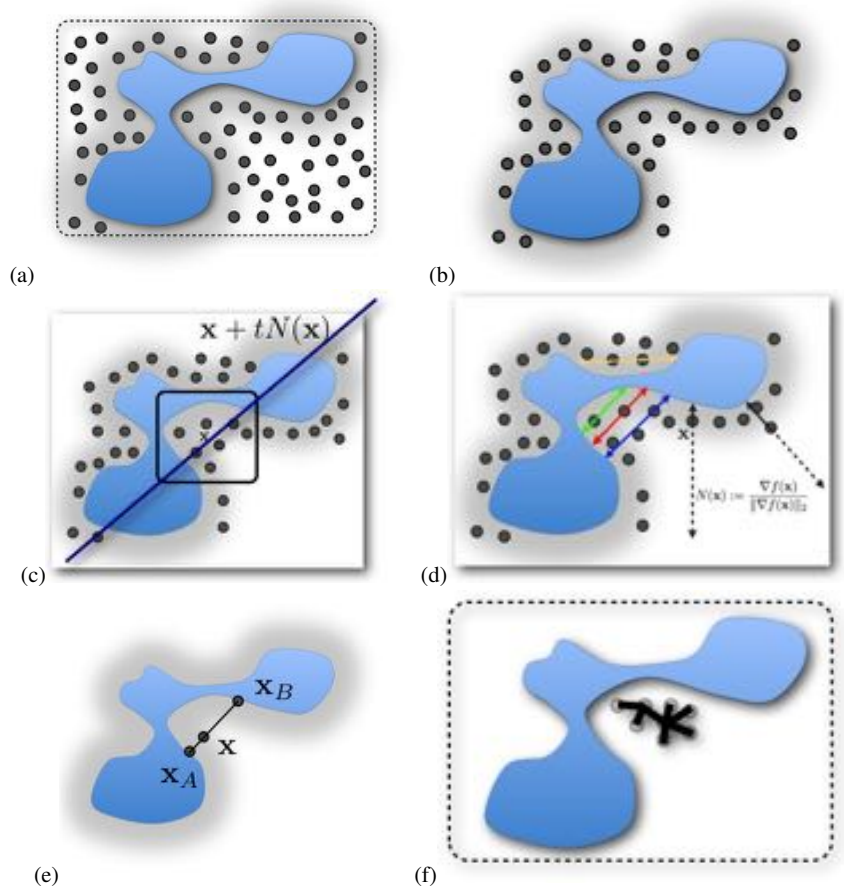

Fig. 1.8: ***Exploration and characterization of molecular cavities***. *(a) Bounding box of the molecular surface $\mathscr{S}$ and random samples; (b) identification of those samples that are outside $\mathscr{S}$ and whose distance from $\mathscr{S}$ is lower than $d := 2r$, where r is the probe radius. (c, d) Rays $\mathbf{x} + D\mathbf{N}(\mathbf{x})$ through each sample $\mathbf{x}$ along the normal to the molecular surface and its intersection with the molecular surface. (e) Intersection points $\mathbf{x}_A$ and $\mathbf{x}_B$ between the molecular surface and the ray traced through $\mathbf{x}$. (f) Cavity graph defined as the undirected graph associated to the mid-points of $\mathbf{x}_A$, $\mathbf{x}_B$ previously computed.*

ture is small with respect to the local sampling distance. Under specific assumptions on the regularity of $\mathscr{A}$, we can guarantee the smoothness of the signed point-to-set distance. More precisely, if $\mathscr{A}$ is a closed subset with a piecewise smooth boundary then the signed point-to-set distance is differentiable almost everywhere and its gradient satisfies the eikonal equation.

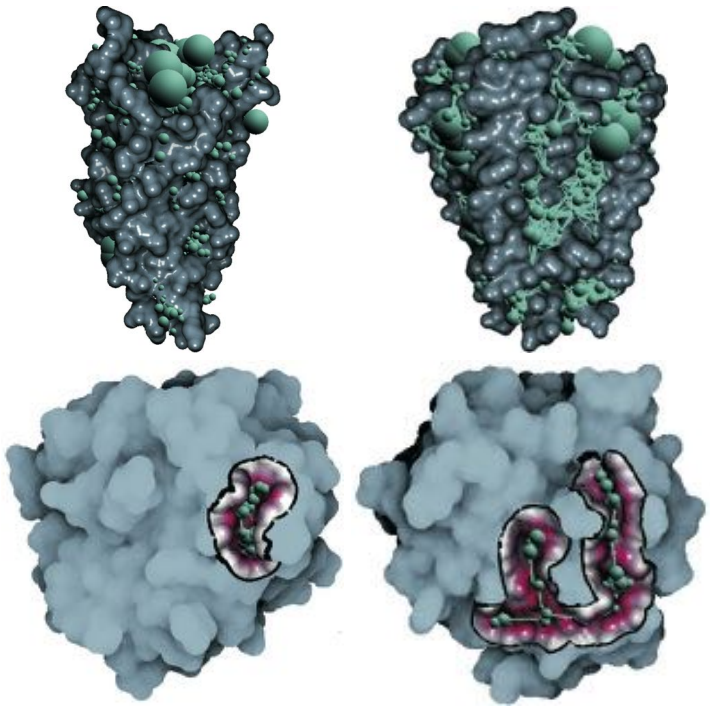

Fig. 1.9: ***Molecular cavities.*** *Cavities' graphs on molecular surfaces. Image courtesy of [19].*

Signed point-to-set distance In several applications (e.g., cavities exploration in molecular surfaces), it is useful to distinguish points outside and inside the molecular surface. For instance, the definition of the molecular surface with CSG operations (Sect. 1.3) uses an analogous implicit function. To this end, we consider the signed point-to-set distance, which is a variation of the point-to-set distance and is defined as (Fig. 1.7(c))

$$d(\mathbf{x},\mathscr{A}) := \begin{cases} d(\mathbf{x},\mathscr{A}^C), & \mathbf{x} \in \mathscr{A}, \\ -d(\mathbf{x},\mathscr{A}), & \mathbf{x} \in \mathscr{A}^C. \end{cases}$$

According to this definition, the signed point-to-set distance is positive inside the set $\mathscr{A}$, negative outside $\mathscr{A}$, and null on $\mathscr{A}$. The *signed distance field* $f : \mathbb{R}^d \to \mathbb{R}$ can also be defined through the eikonal equation $\|\nabla f\|_2 = 1$ and the condition of the zero set $f|_{\mathscr{S}} = 0$. The signed point-to-set distance is a continuous function and its derivatives are defined almost everywhere; i.e., with the exception of those points of $\mathbb{R}^d$ that have no unique closest surface points.

We now characterize the point-to-set distance to the iso-surface of an implicit function $f : \mathbb{R}^d \to \mathbb{R}$ by understanding the relation between the value $f(\mathbf{x})$ and the point-to-set distance of $\mathbf{x}$ from the iso-surface $f^{-1}(0)$ (Fig. 1.7(d)). In general, it is not true

that $f(\mathbf{x})$ is equal to the point-to-set distance of $\mathbf{x}$ from $f^{-1}(0)$. For instance, if we multiply f by a non-null constant α then αf has the same iso-surface of f for the null iso-value and the same point-to-set distance function; however, the values of f and αf at $\mathbf{x}$ are different, $\alpha \neq 1$. Indeed, we need to introduce some assumptions on the values of f and its smoothness in order to characterize the relation between the value $f(\mathbf{x})$ and the distance of $\mathbf{x}$ from the iso-surface $f^{-1}(0)$. According to [10], let us assume that f is a Lipschitz function; i.e., there exists a constant Lip_f such that $|f(\mathbf{x}) - f(\mathbf{y})| \leq \mathrm{Lip}_f \|\mathbf{x} - \mathbf{y}\|_2$. After the normalization of f with the Lipschitz constant, $|f(\mathbf{x})/\mathrm{Lip}_f|$ is lower than the point-to-set distance of $\mathbf{x}$ from the level-set $f^{-1}(0)$; i.e.,

$$\left| \frac{f(\mathbf{x})}{\mathrm{Lip}_f} \right| \leq d(\mathbf{x}, f^{-1}(0)). \tag{1.4}$$

Since the implicit function underlying the blobby model is Lipschitz, it satisfies the upper bound (1.4) to the point-to-set distance. After the normalization of the blobbly implicit function with respect to its Lipschitz constant, Eq. (1.4) gives a simple way to estimate the distance of a point $\mathbf{x}$ from the molecular surface. Finally, the solvent excluded surface is computed locally and the implicit function provides the minimal distance to $\mathscr{S}$.

1.5.2 Cavities' exploration for molecular docking

In the following, we discuss a simple and effective method to identify the cavities of molecular surfaces [19], which is important for a better characterization of the geometry of the molecular surface and the support to molecular docking [4, 18, 26].

First of all (Fig. 1.8(a)), we identify the bounding box of the molecular surface and we sample s random points in this box and select $d := 2r$ as the maximum distance between the molecular surface and the sample $\mathbf{x}$. Then, we remove all those samples that are inside the molecular surface or whose point-to-set distance from the molecular surface is greater than a given threshold, which is set equal to $2r$, where r is the probe radius (Fig. 1.8(b)). Using the CSG model for the molecular surface, these two conditions are simply evaluated by sampling the implicit function at the samples and checking if these two conditions are satisfied or if they are not fulfilled.

In the selected set of samples, we identify samples belonging to potential cavities by casting a ray $\mathbf{x} + D\mathbf{N}(\mathbf{x})$ through each sample $\mathbf{x}$ along the normal to the molecular surface (i.e., using the gradient of the implicit function) and studying its intersection with the molecular surface (Fig. 1.8(c,d)). More precisely, we need to solve the non-linear equation $f(\mathbf{x} + D\mathbf{N}(\mathbf{x})) = 0$. To verify if this predicate is satisfied, we apply a ray-tracing procedure or an iterative solver. In the first case, the time parameter is incremented until the molecular surface is pierced by the ray and this procedure is the same used for the visualization of the iso-surfaces of implicit maps. In the

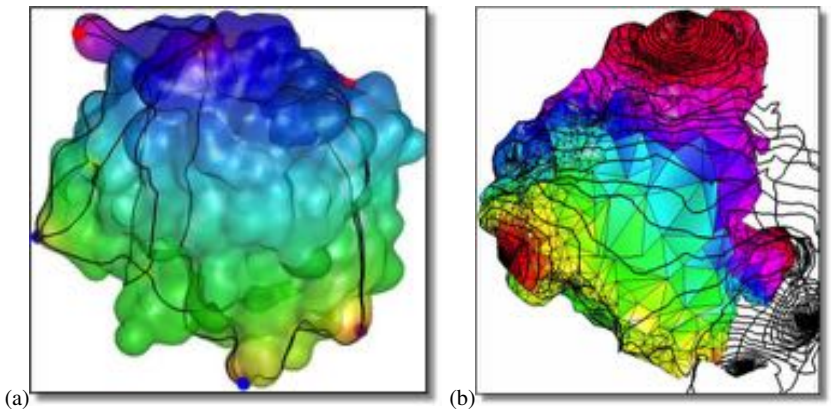

Fig. 1.10: ***Morse complex and volumetric sampling of the electron density map.*** *(a) Morse complex and critical points of the curvature values on a molecular surface. Maxima, minima, and saddles are represented as red, blue, and green points. (b) Volumetric sampling of the density map induced by the interaction of this molecule with surrounding molecules [28].*

second case, the iterative solver approximates the solution to the non-linear equation by locally linearizing it.

Let us assume that we have identified two points $\mathbf{x}_A$ and $\mathbf{x}_B$ of intersection between the molecular surface and the ray traced through the sample point $\mathbf{x}$ (Fig. 1.8(e)). By definition, one of these two points (i.e., the one closest to the molecular surface) is identified by the point-to-set distance. Then, we replace $\mathbf{x}$, $\mathbf{x}_A$, and $\mathbf{x}_B$ with the mid point between $\mathbf{x}_A$ and $\mathbf{x}_B$. We then compute the cavity graph as an undirected graph of these new points (Fig. 1.8(f)), where an edge of the graph exists if there is no surface between the two endpoints. Fig. 1.9 shows the cavities' graphs of different molecular surfaces.

1.6 Discussion and future work

The correct representation of molecular surfaces is fundamental for their processing, analysis, and visualization. However, multiple connected components, spurious cavities or holes, and topological inconsistencies affect the current representations of molecular surfaces. A locally incorrect representation of the molecular surface wrongly influences the classification of its features, the identification of docking sites, and the evaluation of local similarities among molecules. These geometric and topological artifacts in the representation of the molecular surfaces [1] are also due to the resolution of the voxel grid, on which the electrostatic field is sampled

to extract the molecular surface through Marching Cubes [13] or alternative algorithms [9]; local perturbations in the computed samples of the electron density map; numerical errors; and a limited approximation accuracy. A locally incorrect representation of molecules, which is due to inherent pathologies in the classical definition of the van der Walls, solvent-accessible and solvent-excluded surfaces, badly influences the classification of its features, the identification of docking sites, and the evaluation of local similarities among molecules. These geometric and topological artifacts in the molecular surface representation are generally due to the resolution of the voxel grid used by the Marching Cubes, local perturbations in the computed samples of the electron density map, numerical errors, or limited approximation accuracy.

In this context, we have reviewed implicit modeling techniques for the representation, analysis, and characterization of the electron density map and the underlying molecular surface, with possible applications to the analysis of molecular cavities for docking. Even though the definition of a correct representation of the molecular surface is still crucial to correctly simulate the mutual interactions of molecules and the understanding of biological phenomena, a unique definition of the molecular surface, which combines all its main properties, is still missing. Recent definition of the molecular surface, which take into account the vibration of the atoms and their fuzzy location in space, are promising to address complex problems, such as the study of the interactions among molecular and molecular docking.

The possibility of sampling the electron density map at the nodes of a volumetric grid has allowed us to combine surface-based and volume-based information. Fig. 1.10 shows a color coding of the values of the electron density map at the nodes of a tetrahedral mesh generated staring from a triangle mesh of the molecular surface (e.g., [7]). Considering the class of molecular surfaces defined through implicit representations, discrete and continuous differential properties [14] of the electron density map, such as the critical points classification and distribution, can be used to automatically identify, classify, and remove degeneracies and inconsistencies during the computation of the molecular surface. This discussion can be applied to both discrete and continuous electron density maps, such as the blobby model [28], implicit representations [19], the Connolly surface [5]. Indeed, as future work we plan to investigate the analysis of degeneracies in molecular surfaces through differential properties of implicit functions with the final aim of validating those methods of differential geometry that are meaningful from the biophysics perspective and are useful for the extraction of a molecular surface that is free of topological noise and geometric artifacts.

Acknowledgements This work has been partially supported by the Italian Flagship Project *Interomics* and the Research Project "*Methods and Techniques for the Development of Innovative Systems for Modeling and Analyzing Biomedical Data for Supporting Assisted Diagnosis*", PO CRO Programme, European Social Funding Scheme, Regione Liguria.

References

1. C. Bajaj, A. Gillette, and S. Goswami. Topology based selection and curation of level sets. In *Topology-Based Methods in Visualization II*, Mathematics and Visualization, pages 45–58. Springer Berlin Heidelberg, 2009.
2. J. F. Blinn. A generalization of algebraic surface drawing. *ACM Transactions on Graphics*, 1(3):235–256, 1982.
3. J. C. Carr, R. K. Beatson, J. B. Cherrie, T. J. Mitchell, W. R. Fright, B. C. McCallum, and T. R. Evans. Reconstruction and representation of 3D objects with radial basis functions. In *ACM Siggraph*, pages 67–76, 2001.
4. B. Y. Chen and B. Honig. Vasp: A volumetric analysis of surface properties yields insights into protein-ligand binding specificity. *PLoS Comput. Biol.*, 6(8):e1000881, 08 2010.
5. M. L. Connolly. Analytical molecular surface calculation. *Journal of Applied Crystallography*, 16(5):548–558, 1983.
6. S. Decherchi, J. Colmenares, C. E. Catalano, M. Spagnuolo E. Alexov, and W. Rocchia. Between algorithm and model: Different molecular surface definitions for the poisson-boltzmann based electrostatic characterization of biomolecules in solution. *Communications in Computational Physics*, 13:61–89, 2013.
7. S. E.D. Dias and A. J.P. Gomes. Graphics processing unit-based triangulations of blinn molecular surfaces. *Concurrency and Computation: Practice and Experience*, 23(17):2280–2291, 2011.
8. R. Farwig. Multivariate interpolation of arbitrarily spaced data by moving least squares methods. *Journal of Computational and Applied Mathematics*, 16(1):79–93, 1986.
9. A. Gomes, I. Voiculescu, J. Jorge, B. Wyvill, and C. Galbraith. *Implicit Curves and Surfaces: Mathematics, Data Structures and Algorithms*. Springer Publishing Company, Incorporated, 1st edition, 2009.
10. J. C. Hart. Sphere tracing: a geometric method for the antialiased ray tracing of implicit surfaces. *The Visual Computer*, 12(10):527–545, 1996.
11. C. H. Lee and A. Varshney. Representing thermal vibrations and uncertainty in molecular surfaces. *Proc. SPIE*, 4665:80–90, 2002.
12. D. Levin. The approximation power of moving least-squares. *Mathematics of Computation*, 67(224):1517–1531, 1998.
13. W. E. Lorensen and H. E. Cline. Marching cubes: A high resolution 3D surface construction algorithm. *ACM SIGGRAPH Computer Graphics*, 21(4):163–169, 1987.
14. J. Milnor. *Morse Theory*, volume 51 of *Annals of Mathematics Studies*. Princeton University Press, 1963.
15. B. S. Morse, T. S. Yoo, D. T. Chen, P. Rheingans, and K. R. Subramanian. Interpolating implicit surfaces from scattered surface data using compactly supported radial basis functions. In *IEEE Shape Modeling and Applications*, pages 89–98, 2001.
16. Y. Ohtake, A. Belyaev, M. Alexa, G. Turk, and H.-P. Seidel. Multi-level partition of unity implicits. *ACM Siggraph*, 22(3):463–470, 2003.
17. Y. Ohtake, A. Belyaev, and H.-P. Seidel. 3D scattered data interpolation and approximation with multilevel compactly supported RBFs. *Graphical Models*, 67(3):150–165, 2005.
18. J. Parulek and A. Brambilla. Fast blending scheme for molecular surface representation. *IEEE Transactions on Visualization and Computer Graphics*, page to appear, 2013.
19. J. Parulek, C. Turkay, N. Reuter, and I. Viola. Implicit surfaces for interactive graph based cavity analysis of molecular simulations. In *2nd IEEE Symposium on Biological Data Visualization*, 2012.
20. J. Parulek and I. Viola. Implicit representation of molecular surfaces. In *IEEE Pacific Visualization Symposium*, pages 217–224, 2012.
21. A. Pasko, V. Adzhiev, A. Sourin, and V. Savchenko. Function representation in geometric modeling: concepts, implementation and applications. *The Visual Computer*, 11(8):429–446, 1995.

22. M. Pauly, R. Keiser, L. P. Kobbelt, and M. Gross. Shape modeling with point-sampled geometry. *ACM Transactions on Graphics*, 22(3):641–650, 2003.
23. A. Ricci. A constructive geometry for computer graphics. *The Computer Journal*, 16(2):157–160, 1973.
24. G. Turk and J. F. O'Brien. Modelling with implicit surfaces that interpolate. *ACM Siggraph*, 21(4):855–873, 2002.
25. H. Wendland. Real piecewise polynomial, positive definite and compactly supported radial functions of minimal degree. *Advances in Computational Mathematics*, 4(4):389–396, 1995.
26. Zhang X. and Bajaj C. Extraction, quantification and visualization of protein pockets. *Comput Syst Bioinformatics Conf.*, (6):275–286, 2007.
27. H. Xie, K. T. McDonnell, and H. Qin. Surface reconstruction of noisy and defective data sets. In *IEEE Visualization*, pages 259–266, 2004.
28. Y. Zhang, G. Xu, and C. Bajaj. Quality meshing of implicit solvation models of biomolecular structures. *Computer Aided Geometric Design*, 23(6):21, 2006.